RSC Applied Polymers

PAPER

View Article Online
View Journal | View Issue

Cite this: *RSC Appl. Polym.*, 2026, **4**, 345

Material extrusion additive manufacturing of wood pulp-reinforced epoxy composites

Meghan E. Lamm, *[a] Katie Copenhaver, [a] Tyler Smith,[a] Madeline G. Wimmer, [b] Greg Larsen, [a] Brett G. Compton [b,c,d] and Halil Tekinalp[a]

Received 15th October 2025,
Accepted 20th November 2025

DOI: 10.1039/d5lp00325c

rsc.li/rscapplpolym

Direct ink writing (DIW) is an extrusion-based form of 3D-printing that has gained popularity over the last decade. DIW uses thixotropic fluid extrusion to form a particular shape. In order to form stable structures, the rheology of the paste is important to allow for extrusion from the syringe, stability of the growing print, and prevention of unwanted seeping flow during jog moves. In this work, we use wood pulp as a bio-based filler that can provide shear thinning properties to the ink, which produces a stable ink for DIW processing. Additionally, the filler imparts improved mechanical and thermal performance compared to neat resin. The wood pulp provided the shear thinning behavior necessary for DIW printing, and pulp loadings greater than 6 wt%, provided sufficient yield stress so that the composite could self-support during printing. Nanoclay was utilized to further improve ink rheology and appearance to enable larger scale printing. Overall, this work showed successful DIW of an epoxy resin with a sustainable filler improving its stiffness and thermal properties and provides an avenue for further development of bio-based inks for DIW towards various applications.

Introduction

Direct ink writing (DIW) 3D printing is a useful technique to turn thermoset pastes into complex shapes, and it has grown in popularity over the last decade.[1,2] Thermoset materials are more promising in a variety of applications over thermoplastics due to their superior mechanical properties and chemical resistance. However, thermosets typically require more complex processing such as casting, vacuum-assisted resin transfer (VARTM), prepregs or sheet molding compounds, all of which require the use of molds that can be costly and time consuming to make. DIW allows researchers to produce complex shapes without the need for molds or tools, decreasing costs and increasing the applicability of thermoset materials.[3] Compared to 3D-printed thermoplastics, thermosets also feature better interlayer adhesion, arising from direct curing between the layers and intertwining of fillers, which aids in their improved mechanical performance. Unfortunately, thermosets can also struggle to form stable structures, as the thermoset paste in DIW must undergo a chemical reaction before solidifying, not just cooling like thermoplastics. As such, there is a limit to the achievable pre-cure height and aspect ratio in DIW printing before yielding, buckling, or collapse occurs for materials without rapid cure.[4] The rheological behavior of the ink during extrusion and after deposition at rest is very important to the success of the print. The material should exhibit a sufficiently high yield stress to resist unwanted seepage from the nozzle during printing and enable flow of the material only when pressure is applied in the nozzle. Additionally, shear thinning behavior and an efficient recovery of a high viscosity after extrusion (*i.e.*, zero-shear viscosity) is desirable to enable extrusion at the targeted throughput while ensuring dimensional stability of the printed object. Fillers are commonly used to develop the desired rheological profile such that when combined with the cure process (ambient, latent, or *in situ* applied energy), the print will be successful. Some nano- and micro-scale fillers can impart these necessary behaviors, particularly when they feature a high aspect ratio. Clays, carbon fiber, graphene, and other inorganic particles have all been used in literature to achieve printable inks by transforming the Newtonian resin into a shear-thinning paste.[5–8] Furthermore, the fillers can extend new properties in the final composite material, opening an avenue for new applications. For instance, Chi *et al.* incorporated graphene nanoplatelets into an epoxy resin and imparted electrical and thermal conductivity into the finished material.[9] These fillers can also improve mechanical and thermal performance of the thermoset due to alignment of the fibers during printing.[10]

[a]*Manufacturing Science Division, Oak Ridge National Laboratory, Oak Ridge, TN, 37830, USA. E-mail: lammme@ornl.gov*
[b]*University of Tennessee-Oak Ridge Innovation Institute, Knoxville, TN 37996, USA*
[c]*Mechanical and Aerospace Engineering Department, University of Tennessee, Knoxville, TN 37996, USA*
[d]*Materials Science and Engineering Department, University of Tennessee, TN 37996, USA*

Bio-based alternatives to these established DIW ink fillers are being explored due their low embodied energy and similar performance. For example, wood pulp, sawdust, and cellulose nanomaterials have all been reported as fillers in polymer composites.[11] Wood pulp and other wood-based materials have been incorporated into thermoset composites, similar to commercial wood glue, but they feature a low aspect ratio and tend to only achieve parity in mechanical properties to neat resins.[12–14] Comparatively, wood pulp has been used in the 3D-printing of thermoplastics with a resulting improvement in mechanical performance.[15,16] Due to its high aspect ratio, wood pulp aligns with the flow of material during extrusion, accounting for the improved performance seen in these studies. Wood pulp has also been proven to impart shear thinning behavior in thermoplastic composites during thermoplastic 3D-printing, and it stands to reason that a similar effect would be obtained for a thermoset system reinforced with wood pulp.[17] It is worth noting that bio-based alternatives to the thermoset materials in DIW inks are also being explored to produce greener inks, such as those derived from vegetable oils, lignin, and even resin acids. Some of these materials also impart unique functionality into the final materials, including the presence of dynamic bonding which imparts recyclability, however these areas are outside the scope of this work.[18–21] In this study, wood pulp is incorporated into an epoxy matrix and processed using DIW. The rheological behavior of the ink formulations is studied extensively to optimize its printability and resulting properties. Overall, the wood pulp imparts the necessary rheological behavior needed for success in DIW while improving the thermal and mechanical performance of the epoxy composite, opening the way for new applications of bio-based thermoset composites.

Experimental

Materials

Epirez WD510, a bisphenol-A epoxy resin containing an added surfactant, and Epikure 3274 were purchased from Hexion. CreaTech TC 750, a dried wood pulp, was purchased from Creafill Fibers Incorporated. The wood pulp chosen for this work features a length of around 750 microns and a width less than 50 microns (Fig. S1). Garamite 7305 clay was provided by BYK USA.

Preparation of thermoset composites

Epirez WD510, Epikure 3274, wood pulp, and clay were weighed out in a cup. The cup was then placed in a FlackTek mixer and mixed at the following conditions: 45 s at 800 rpm, 30 s at 1200 rpm, and 1 min at 1800 rpm under vacuum. The FlackTek mixer both combine the reagents and degas them under vacuum. The ratio of epoxy to hardener was kept at 100 parts to 37 parts. Ratios of the wood pulp and clay were varied in the inks between 0–10 wt% wood pulp, according to the compositions needed in the final formulation. After mixing, the mixture was loaded into a syringe for printing or into a silicone mold for ASTM D638 type V tensile bar formation. Filled resins were too viscous for casting and were printed, while neat resin was cast. The samples cured at room temperature for 72 h.

Additive manufacturing

Thermoset additive manufacturing has been completed using methods such as DIW, extrusion deposition, and plunger/syringe-based deposition. For small scale tests, a Makergear M2 was converted to a thermoset printed by adding a 30cc syringe in place of the hot end to enable small scale thermoset deposition tests. The system used a 1.3 mm nozzle and a 0.6 mm bead height. A 2-part epoxy system was pre-mixed and then loaded into the syringe to deposit the material for testing. Mixing and deposition was completed prior to the time required for crosslinking to occur. The shape shown in Fig. S2 was prepared to test stability and homogeneity of the composite mixture. Larger scale studies were performed on an Orbital Composites 3D printing system. The system utilized a 16 oz syringe, 4 mm nozzle, and 4 mm bead height. Printing occurred with a Q of 203.2 $mm^3\ s^{-1}$, a linear speed of 12.7 mm s^{-1} and a plunge rate of 0.07 mm s^{-1}. A triangular prism composed of three 5 × 3-inch faces were printed, shown in Fig. S3. The triangle was printed to ~1 inch in height at a time to prevent sagging, as shown in Fig. 3. Each layer was given 2 h to gel. ASTM D638 Type V tensile bars and ASTM E831 CTE cubes were milled in the *X*-direction of the triangular prism faces, as shown in Fig. S3.

Characterization of composite samples

Tensile properties were measured by using the dog-bone specimens tested at room temperature *via* a servo-hydraulic testing machine (MTS Criterion Model 45) with a 10 kN load cell at a speed of 1.5 mm min^{-1}. The strain on each sample was monitored using an extensometer. Four specimens for each sample were tested, and the average was reported. The cross-sectional morphology of the composite samples after fracture was imaged using a Zeiss Merlin VP high-resolution field-emission type scanning electron microscope (SEM) operating at an accelerating voltage of 1 kV. Differential scanning calorimetry (DSC) was performed using a TA Instruments Q2000 apparatus using heat/cool/heat mode to remove residual heat stress prior to determining thermal transitions. The scanning conditions were set as follows: each sample was first equilibrated at 25 °C followed by heating to 200 °C at a rate of 10 °C min^{-1} before allowing it to cool at the same rate to 25 °C. During the second heating cycle the sample was heated again to 200 °C at 10 °C min^{-1}. Thermal mechanical analysis (TMA) of the composites was performed on a TA Instruments (TMA450) apparatus using a macroexpansion probe to determine each sample's coefficient of thermal expansion (CTE). The test samples consisted of 10 mm × 10 mm × 10 mm cubes. A preload force of 0.05 N was used. The samples were equilibrated at 25 °C using 0.1 N of force, then heated to 135 °C at a rate of 3 °C min^{-1}. Four replicate samples were collected for each material. The Vicat softening temperature was also determined by TMA using a

penetration probe. A preload force of 0.05 N was used to load a sample of 10 mm × 10 mm × 10 mm. The force was raised to 200 g while being heated at 5 °C min^{-1} up to 135 °C. Three replicate samples were collected for each material. The materials' rheological behavior was studied using a TA Instruments ARES-G2 rheometer. Samples were tested within 1 h of mixing to prevent effects of aging or initial curing. Each test used 25 mm disposable aluminum parallel plates. As the ARES-G2 rheometer is strain-controlled, oscillatory strain sweeps were performed and converted to stress *vs.* modulus data to determine the sample's yield behavior. The strain sweeps were conducted on each material at ambient temperature from 0.01 to 200% strain at an angular frequency of 1 rad s^{-1}. Steady shear tests were then conducted to determine the viscosity of each sample with respect to shear rate. Tests were performed at shear rates from 0.01 to 100 s^{-1} but were truncated if strain localization was observed or the material began to flow out from between the platens. The thermal degradation behavior was determined by thermogravimetric analysis (TGA) using a TA Instruments Q500 apparatus. The samples were heated from room temperature to 700 °C at a ramp rate of 10 °C min^{-1} under air flow.

Results and discussion

The flow behavior of epoxy-based DIW inks with a range of wood pulp filler was first analyzed using steady shear. The wood pulp content was increased from 0 to 10 wt% in increments of 2 wt%. As shown in Fig. 1, the viscosity of each formulation increased with wood pulp content across all the range of shear rates investigated. Furthermore, each composite ink demonstrated non-Newtonian shear thinning behavior, while the neat resin displayed no shear thinning, with viscosity independent of shear rate. At wood pulp contents above 4 wt%, the shear thinning behavior further improved, indicated by the steeper slope of samples with 6–10 wt% of wood pulp as compared to those with 2 and 4 wt%. This change in behavior could be attributable to a critical concentration of pulp fiber beyond which fiber-fiber interactions dominate viscoelastic behavior and potentially form a network within the composite (*i.e.*, percolation threshold). It should be noted that the higher filled samples exhibited wall slip at high shear rates. Specifically, the ink containing 10 wt% wood pulp was viscous enough to be free-standing and was observed to slip off the plates around 12 s^{-1}. As such, the data shown in Fig. 1 is truncated to 12 s^{-1}.

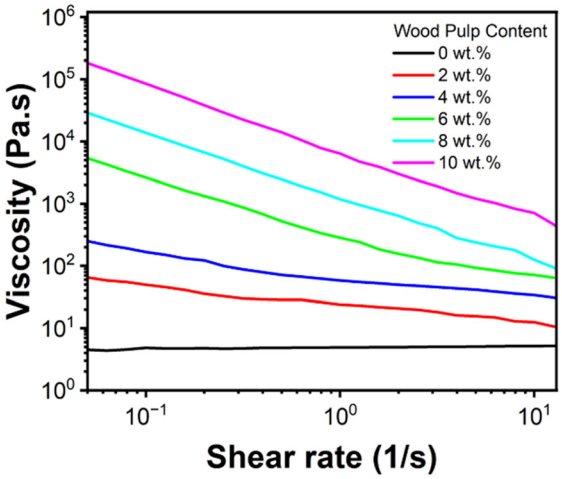

Fig. 1 Flow studies on epoxy composite inks featuring various levels of wood pulp.

Each formulation was then subjected to an oscillatory strain sweep to investigate its yielding behavior. The oscillation stress and shear moduli were measured during each experiment and are plotted in Fig. 2. In these plots, the plateau modulus can be defined as the plateau in storage modulus (G') at low oscillation stress. Additionally, the shear yield stress can be determined as the onset point of a decrease in the storage modulus with respect to oscillation stress. Materials displaying a plateau modulus and yield point can essentially function as a solid below a certain stress threshold, after which they yield and can exhibit non-Newtonian flow with increasing stress. A higher plateau modulus also indicates that the material is stiffer while at rest, and a high yield stress indicates the material can withstand a large amount of stress before yielding, which can be thought of in terms of pressure in a nozzle or the weight of a printed object on the lower layers. Both properties are desirable in DIW for avoiding drippage from the nozzle when extrusion is stopped and for stability of the printed object as its height (*i.e.*, number of layers) increases. As a solid-like behavior is desired in the plateau region, the storage modulus should exceed the loss modulus (G''). Both the neat resin and 2 wt% wood pulp sample displayed a loss modulus greater than the storage modulus across the range of strain rates (converted to oscillation stress in Fig. 2) tested, making them a poor choice for DIW. Likewise, 4 wt% wood pulp displays a low shear yield stress, below 10 Pa, and 6 wt% wood pulp also showed a low value, around 100 Pa. Once at 8 wt% wood pulp or above, the shear yield stress is above 1000 Pa, and is therefore likely stable enough under high stress that it could support printing. Further increase in filler content is not necessary as a higher shear yield stress could result in an ink that is too viscous and could damage the printing equipment, likewise it produced little increase in plateau modulus, indicating an increase was not needed. To test the printability of the recommended 8 wt% wood pulp ink, small test samples were produced (Fig. S2). These test samples were around 2 inches in length and 1 inch width. These samples were easy to print, experienced no nozzle clogging, and did not sag during or after printing. It was also determined that the ink gelled in about 2 hours, at which point it was no longer able to flow and print, which was faster than the 8–9 hours noted by the manufacturer, likely due to the increased viscosity imparted by the filler.

A larger sample was then printed using the 8 wt% wood pulp ink to prepare samples for thermal and mechanical

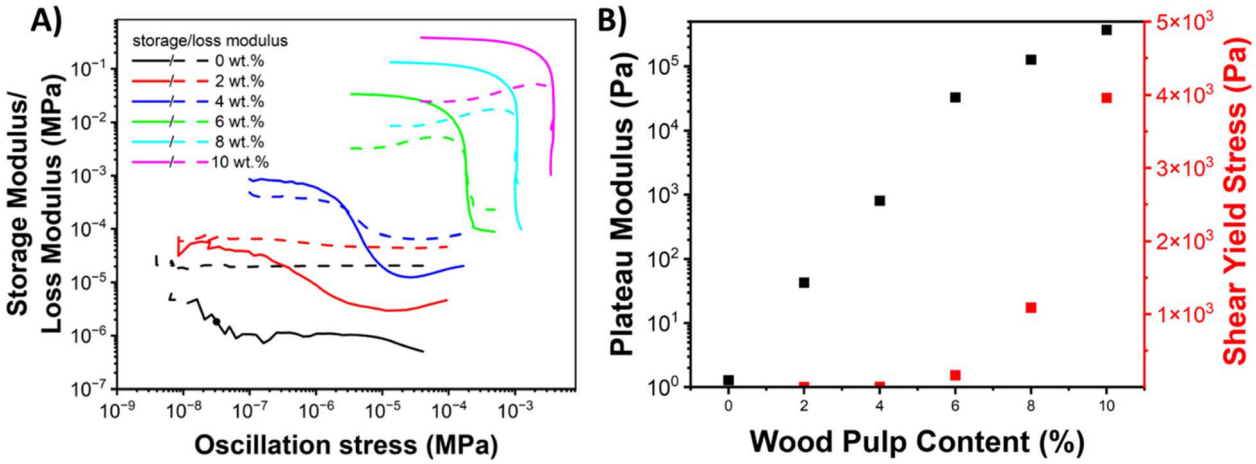

Fig. 2 Rheological studies on the epoxy composites including a stress sweep and its corresponding (A) storage (G') and loss modulus (G'') at varying oscillation stress and (B) plateau modulus and shear yield stress at varying wood pulp content.

testing. A triangle featuring 5 × 3-inch panels at each face was chosen for printing, as the size was sufficient to produce Type V tensile dogbones at each face (Fig. S3). The first print attempt featured no infill pattern and failed around 1 inch of height due to sagging and collapse of the walls. This height is close to the limit reached for a 2 bead wall before failure with other DIW systems reported in literature.[4] Additionally, the viscosity of the ink made it difficult to print on the larger scale system and resulted in bending of the syringe fixture and the creation of air bubbles in the print. The anomalous behavior between the small benchtop printer used in initial trials and the larger scale system used to print the triangle sample could be attributed to differences in equipment design as well as the inherent higher pressures and shear rates needed to extrude a larger amount of material at a higher throughput. It was determined that a lower viscosity ink was needed for printing on the larger system. In order to preserve a higher bio-based reinforcement content in the composite, nanoclay was added to the ink formulation. Nanoclay is a common additive in DIW inks and has been shown to improve flow properties and dimensional stability during and after extrusion, respectively, without significantly increasing the ink's viscosity. Based on a survey of other nanoclay-containing DIW inks in literature, a loading of 5 wt% was chosen for addition to the epoxy/wood pulp ink, as a loading of 5 wt% or less was shown useful in reinforcing the ink and providing adequate rheological improvement.[22–24]

The rheological properties of the new ink with 8 wt% wood pulp and 5 wt% nanoclay were then characterized and are shown in Fig. S7 and S8 in the SI. The new ink displayed a reduced viscosity profile in steady shear at low shear rates and slightly higher viscosity at high shear rates in comparison to the ink without nanoclay. The nanoclay-containing ink exhibited the desired shear thinning behavior, but the degree of shear thinning in the nanoclay/wood pulp ink was lower than that of the wood pulp ink, exhibited by a lower slope of the nanoclay ink in the viscosity-shear rate plot (Fig. S7). The ink also displayed a slight decrease in plateau modulus and notable decrease in the yield stress (Fig. S8), around an order of magnitude decrease each, respectively. However, it is known that nanoclays, unlike some other fillers, form an aligned network within their composite matrix during DIW, so there was little concern with the decrease in properties resulting in any complications during printing.[25] Additionally, it is worth noting that the nanoclay produced a far more homogenous, smoother ink, despite containing the same amount of wood pulp as the previous ink. The triangle was reprinted on the larger orbital system using the new ink with nanoclay. An initial print following the previous procedure was attempted with this new ink; however, it also failed, albeit at a greater wall height around 1.75 inches. Therefore, an infill pattern was incorporated into the design to further improve the stability of the print, and the sample was printed about 12 layers at a time (~1 inch in height) and given 2 hours to gel, after which a second section was printed. This process was repeated 3 times, resulting in a final part approximately 3 inches in height. The presence of nanoclay in the ink enabled extrusion without bending of the apparatus, an issue seen in previous prints, due to its decreased viscosity, with a visually more homogenous extrudate. This final sample geometry provided a successful print without sagging (Fig. 3).

The wood pulp was theorized to both impart shear thinning behavior in the ink formulations as well as improve the thermal and mechanical properties of the resulting composite. The performance of the neat resin was then compared to the printed formulation (8 wt% wood pulp and 5 wt% nanoclay) using samples cast to molds from neat resin and samples machined from the print of the composite ink (in the printing direction). The tensile properties of both materials were tested, and results are shown in Fig. 4. The tensile strength was observed to decrease approximately 30% with the incorporation of filler, while the modulus more than doubled.

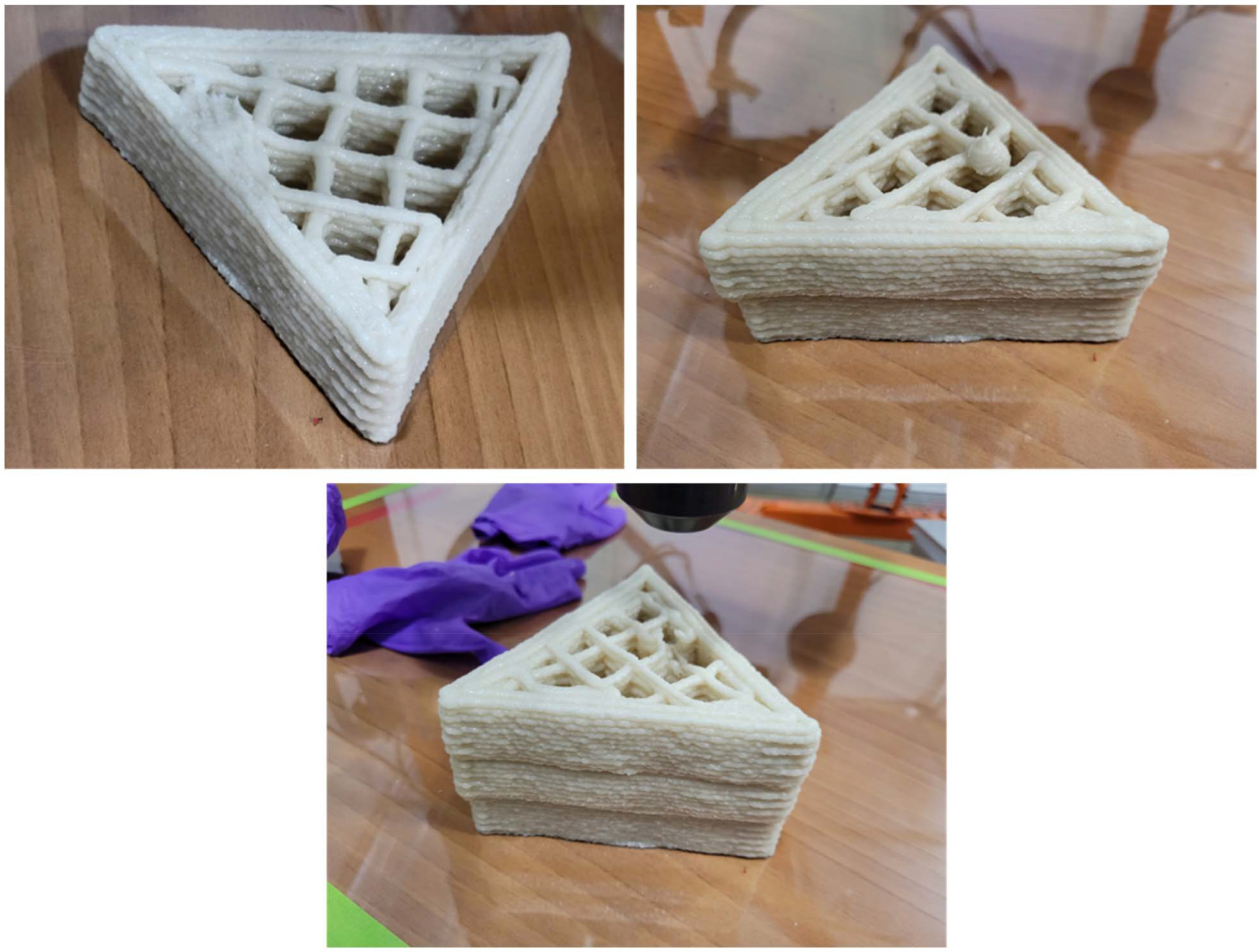

Fig. 3 Large scale triangular samples prepared using the wood pulp and nanoclay filled ink, featuring 5 × 3 inch sides.

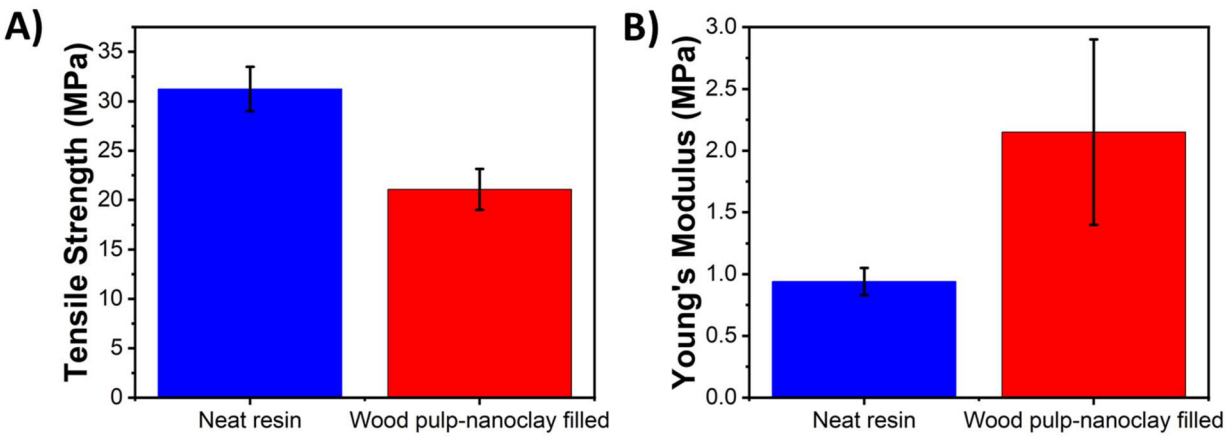

Fig. 4 Tensile properties of the neat resin *versus* the wood pulp and Garamite filled resin including (A) tensile strength and (B) Young's modulus.

Although the wood fibers likely aligned with the flow direction during printing, the decrease in performance is likely attributable to the presence of air pockets throughout the printed sample, as seen in Fig. 5A. The increase in tensile modulus is attributable to the fillers providing an increased stiffness, a common phenomenon for composite materials.[26] Analysis of the samples' fracture surfaces showed the wood pulp and nanoclay dispersed well in the epoxy matrix (Fig. 5B), with

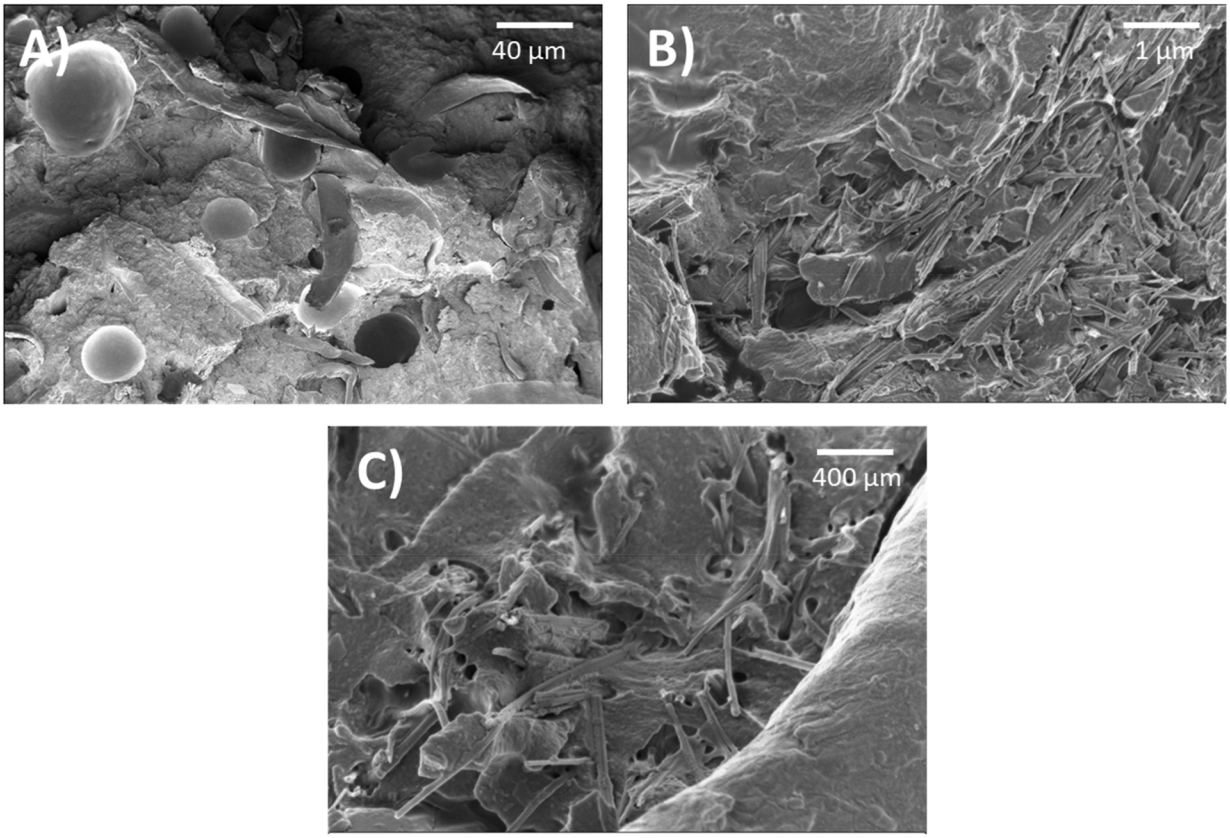

Fig. 5 SEM images of the fracture surface of printed wood-pulp and nanoclay (Garamite) filled resin featuring (A) voids due to printing and the presence of wood pulp, and (B/C) fiber and nanoclay pull out.

some fiber pull out noted in Fig. 5C, indicating the failure occurs at the interface between the filler and the matrix, likely due to stress concentrations located at the interface.

The coefficient of thermal expansion (CTE) and Vicat softening point of the neat and composite materials was then measured. The CTE both in the glassy and rubbery regions was reduced in the filled sample (Table 1) in comparison to that of the neat material. This is consistent with literature as well as the composite's increased modulus, as the fillers are theorized to prevent warpage of the material.[27] Similarly, the Vicat softening point of the neat resin was lower than that of the composite, shown in Table 1, which is consistent with the CTE and tensile modulus trends. The softening point values were similar to the glass transition temperatures (T_g) of each material (Fig. S7). The Vicat softening points of the neat and composite materials were 59 and 67 °C, respectively, while the T_gs were found to be 57 and 66 °C, respectively. The presence of filler in the composite samples likely restricts molecular movement, evidenced by the modulus, CTE, softening, and glass transition behaviors. Additionally, the presence of filler improved the material's thermal stability. The filled resin exhibited a 5% decomposition temperature of 277 °C *versus* 183 °C in the neat resin (Fig. S6). This is likely due to the filler content and composition, as cellulose, the primary component in wood pulp, does not degrade until around 300 °C, and nanoclay, which has been shown to increase decomposition temperature in composite materials.[28,29]

Table 1 Coefficient of thermal expansion (CTE) for the neat resin and the filled resin during (A) the glassy region and (B) the rubbery region, and Vicat softening point

Sample	T_g (°C)	CTE glassy region (°C μm m^{-1})	CTE rubbery region (°C μm m^{-1})	Vicat softening point (°C)
Neat resin	57	1.14×10^{-5} ($\pm 1.62 \times 10^{-7}$)	2.26×10^{-5} ($\pm 3.99 \times 10^{-7}$)	59
Wood pulp-nanoclay filled resin	66	8.48×10^{-6} ($\pm 1.21 \times 10^{-7}$)	1.91×10^{-5} ($\pm 3.38 \times 10^{-7}$)	67

Conclusions

Inks for DIW were prepared using an epoxy resin filled with wood pulp. The wood pulp provided the shear thinning behavior necessary for DIW printing, and an adequate yield stress was achievable at pulp loadings greater than 6 wt%, indicating that the composite could self-support during printing. Initial small-scale studies used 8 wt% wood pulp ink, as it remained

flowable compared to higher wood pulp levels and improved the printability of the ink. However, a lower viscosity ink with additional stability after extrusion was found to be necessary for printing on a larger scale. Nanoclay was added to the composite ink, as it provided ample shear thinning and yield stress without causing a further increase in viscosity. Overall, the inclusion of wood pulp and nanoclay was shown to enable successful DIW of the epoxy resin with a sustainable filler and improve its stiffness and thermal properties towards a greater breath of applications.

Conflicts of interest

There are no conflicts to declare.

Data availability

The data supporting this article has been included as part of the supplementary information (SI). See DOI: https://doi.org/10.1039/d5lp00325c.

Acknowledgements

This manuscript has been authored by UT-Battelle, LLC under Contract No. DE-AC05-00OR22725 with the U.S. Department of Energy. The United States Government retains and the publisher, by accepting the article for publication, acknowledges that the United States Government retains a non-exclusive, paid-up, irrevocable, world-wide license to publish or reproduce the published form of this manuscript, or allow others to do so, for United States Government purposes. The Department of Energy will provide public access to these results of federally sponsored research in accordance with the DOE Public Access Plan (https://energy.gov/downloads/doe-public-access-plan). This manuscript has been authored by UT-Battelle, LLC, under contract DE-AC05-00OR22725 with the US Department of Energy (DOE). The authors acknowledge the support from the DOE Office of Energy Efficiency and Renewable Energy, Advanced Materials and Manufacturing Technologies Office, and the Oak Ridge National Laboratory/University of Maine Hub & Spoke Specialized Materials & Manufacturing Alliance for Resilient Technologies (SM2ART) program. Microscopy studies were completed at the Center for Nanophase Materials Sciences, a DOE Office of Science User Facility.

References

1 R. Mahshid, M. N. Isfahani, M. Heidari-Rarani and M. Mirkhalaf, *Composites, Part A*, 2023, **171**, 107584.
2 M. Saadi, A. Maguire, N. T. Pottackal, M. S. H. Thakur, M. M. Ikram, A. J. Hart, P. M. Ajayan and M. M. Rahman, *Adv. Mater.*, 2022, **34**, e2108855.
3 B. R. Wang, Z. M. Zhang, Z. J. Pei, J. J. Qiu and S. R. Wang, *Adv. Compos. Hybrid Mater.*, 2020, **3**, 462–472.
4 S. K. Romberg, M. A. Islam, C. J. Hershey, M. DeVinney, C. E. Duty, V. Kunc and B. G. Compton, *Addit. Manuf.*, 2021, **37**, 101621.
5 N. S. Hmeidat, D. S. Elkins, H. R. Peter, V. Kumar and B. G. Compton, *Composites, Part B*, 2021, **223**, 109122.
6 Z. Y. Chen, M. Y. Zhang, P. G. Ren, Z. Lan, Z. Z. Guo, H. X. Yan, Y. L. Jin and F. Ren, *Chem. Eng. J.*, 2023, **466**, 143086.
7 K. B. Manning, N. Wyatt, L. Hughes, A. Cook, N. H. Giron, E. Martinez, C. G. Campbell and M. C. Celina, *Macromol. Mater. Eng.*, 2019, **304**, 1800511.
8 B. G. Compton, J. K. Wilt, J. W. Kemp, N. S. Hmeidat, S. R. Maness, M. Edmond, S. Wilcenski and J. Taylor, *MRS Commun.*, 2021, **11**, 100–105.
9 H. Chi, Z. Lin, Y. Chen, R. Zheng, H. Qiu, X. Hu and H. Bai, *ACS Appl. Mater. Interfaces*, 2022, **14**, 13758–13767.
10 K. Niendorf and B. Raeymaekers, *Adv. Eng. Mater.*, 2021, **23**, 2001002.
11 J. J. Andrew and H. N. Dhakal, *Composites, Part C*, 2022, **7**, 100220.
12 R. J. Moon, G. T. Schueneman and J. Simonsen, *JOM*, 2016, **68**, 2383–2394.
13 Y. C. Du, T. F. Wu, N. Yan, M. T. Kortschot and R. Farnood, *Composites, Part B*, 2013, **48**, 10–17.
14 J. Trifol, S. Jayaprakash, H. Baniasadi, R. Ajdary, N. Kretzschmar, O. J. Rojas, J. Partanen and J. V. Seppala, *ACS Sustainable Chem. Eng.*, 2021, **9**, 13979–13987.
15 A. Le Duigou, M. Castro, R. Bevan and N. Martin, *Mater. Des.*, 2016, **96**, 106–114.
16 A. Koffi, L. Toubal, M. Jin, D. Koffi, F. Döpper, H. W. Schmidt and C. Neuber, *J. Appl. Polym. Sci.*, 2021, **139**, 51937.
17 S. Bhagia, R. R. Lowden, D. Erdman, M. Rodriguez, B. A. Haga, I. R. M. Solano, N. C. Gallego, Y. Q. Pu, W. Muchero, V. Kunc and A. J. Ragauskas, *Appl. Mater. Today*, 2020, **21**, 100832.
18 Y. Hu, Y. Dai, G. Zhu, Y. Ma, L. Yuan, S. Tong, L. Hu, P. Jia and Y. Zhou, *J. Cleaner Prod.*, 2024, **436**, 140772.
19 X. Liu, Y. Hu, L. Hu, M. Zhang, P. Jia and Y. Zhou, *React. Funct. Polym.*, 2025, **215**, 106359.
20 V. S. D. Voet, J. Guit and K. Loos, *Macromol. Rapid Commun.*, 2021, **42**, 2000475.
21 A. Thorbole, C. Bodhak, P. Sahu and R. K. Gupta, *Polym. Eng. Sci.*, 2024, **64**, 5879–5902.
22 N. S. Hmeidat, J. W. Kemp and B. G. Compton, *Compos. Sci. Technol.*, 2018, **160**, 9–20.
23 M. W. Ho, C. K. Lam, K. T. Lau, D. H. L. Ng and D. Hui, *Compos. Struct.*, 2006, **75**, 415–421.
24 B. G. Compton, N. S. Hmeidat, R. C. Pack, M. F. Heres and J. R. Sangoro, *JOM*, 2018, **70**, 292–297.
25 E. B. Trigg, N. S. Hmeidat, L. M. Smieska, A. R. Woll, B. G. Compton and H. Koerner, *Addit. Manuf.*, 2021, **37**, 101729.

26 X. L. Ji, J. K. Jing, W. Jiang and B. Z. Jiang, *Polym. Eng. Sci.*, 2002, **42**, 983–993.
27 N. Saba and M. Jawaid, *J. Ind. Eng. Chem.*, 2018, **67**, 1–11.
28 Z. N. Azwa, B. F. Yousif, A. C. Manalo and W. Karunasena, *Mater. Design*, 2013, **47**, 424–442.
29 J. Golebiewski and A. Galeski, *Compos. Sci. Technol.*, 2007, **67**, 3442–3447.